QUANTUM-MECHANICAL SIMULATIONS OF INTERACTION OF MANY-ELECTRON QUANTUM SYSTEMS WITH IONIZING LASER PULSES

A.A. Romanov[1,2], A.A. Silaev[1,2], D.A. Smirnova[1], T.S. Sarantseva[1,3], A.A. Minina[1,3], M.V. Frolov[3], N.V. Vvedenskii[1,2]

[1]Institute of Applied Physics, Russian Academy of Sciences, Nizhny Novgorod, Russia;
[2]University of Nizhny Novgorod, Nizhny Novgorod, Russia;
[3]Department of Physics, Voronezh State University, Voronezh, Russia
E-mail: romanov.alexander.al@gmail.com

We develop parallel program for numerical simulation of the interaction of intense laser pulses with many-electron atoms on the basis of the time-dependent Kohn-Sham equations. It is shown that the use of modern computer clusters makes it possible to solve these equations for a wide class of atoms in a relatively small time, determined by the parameters of the laser pulse and electronic configuration of the atom. High accuracy of the numerical code is demonstrated on the example of calculating the high-frequency spectrum of electron current excited during ionization of noble gas atoms by few-cycle laser pulse.

PACS: 52.38.-r, 31.15.ee, 32.80.-t

INTRODUCTION

Interaction of intense laser field with atoms and molecules is accompanied by many different phenomena interesting from the scientific and applied points of view. These phenomena include, in particular, above-threshold ionization [1], which consists in the possibility of absorption of more photons than are required for the ionization; high-order harmonic generation, which is the result of the acceleration of freed electrons and their collisions with the parent ions [2 - 8]. The excited electron currents can also contain a low-frequency component responsible for the generation of radiation with a frequency much lower than the optical ones, in particular, in the terahertz and mid-IR range [9 - 14].

Despite the fact that most of the atoms and molecules are essentially many-electron quantum systems, numerical studies of the above-mentioned ionization-induced phenomena are traditionally based on the single-active-electron approximation. Within the framework of this approximation all the electrons except one are frozen in their orbitals and the field of the parent ion is described by a static potential well. Such models can have high accuracy under certain conditions, but in many problems single-active-electron approximation is inapplicable, since it does not describe a number of essentially many-electron effects, such as the polarization of the atomic system. One of the methods for describing many-electron effects, which is close to the many-electron time-dependent Schrödinger equation, is the time-dependent density functional theory, which has recently been increasingly used in atomic physics and nonlinear optics [15 - 18]. This approach is based on the system of time-dependent Kohn-Sham (TDKS) equations, in which the Hamiltonian for individual orbitals includes the interaction with the atomic nucleus, electron-electron interaction, as well as interaction with the electric field of the laser pulse [17].

This paper is devoted to the development of parallel program for the numerical solution of TDKS equations for *ab initio* simulation of the evolution of many-electron atoms (such as neon, argon, krypton, and other noble gas atoms) during the interaction with an intense laser fields. The algorithm for solving the three-dimension TDKS equations is based on the spherical harmonics expansion of the potential energy and wave functions of orbitals. The increase in performance of the program related to the parallelization of its individual modules is analyzed and the high accuracy of the program is demonstrated.

1. STATEMENT OF THE PROBLEM

Suppose that a many-electron atom interacts with a linearly polarized laser-pulse electric field of strength $\mathbf{E}(t) = \hat{\mathbf{z}}E(t)$, where t is the time. We assume that the intensity and wavelength of the laser pulse correspond to the dipole approximation in which the action of the magnetic field in the calculation of the atom dynamics can be neglected [4]. We also limit ourselves here to the consideration of atoms in which orbitals initially are occupied by electrons of the opposite spin. Due to the weak influence of the magnetic field, the zero spin polarization is conserved during interaction with the laser pulse, therefore TDKS equations describing the dynamics of a many-electron system are written down as follows (here and below, the atomic system of units is used in which $|e| = \hbar = m_e = 1$, where $\hbar$ is the reduced Planck constant, $e = -|e|$ is the charge and m_e is the mass of the electron):

$$i\frac{\partial}{\partial t}\psi_n(\mathbf{r},t) = \hat{H}\psi_n(\mathbf{r},t), \quad n = 1,..., N/2,$$
$$\hat{H} = -\frac{1}{2}\nabla^2 - \frac{Z}{r} + zE(t) + V_{ee}[\rho(\mathbf{r},t)]. \tag{1}$$

Here, ψ_n is the wave function of the n-th TDKS orbital, Z is the nuclear charge, N is the (even) number of electrons, ρ is the electron density, $V_{ee}[\rho(\mathbf{r},t)]$ is the potential of electron-electron interaction. The electron density is related to TDKS orbitals by equality

$$\rho(\mathbf{r},t) = 2\sum_{n=1}^{N/2}\left|\psi_n(\mathbf{r},t)\right|^2. \tag{2}$$

The electron-electron interaction potential consists of the Hartree potential

$$V_H[\rho(\mathbf{r},t)] = \int d^3r' \frac{\rho(\mathbf{r}')}{|\mathbf{r}-\mathbf{r}'|}, \tag{3}$$

describing the electron repulsion in the framework of the mean field, and the exchange-correlation potential V_{xc} for which the spin unpolarized form of LB94 approximation [19] is used

$$V_{xc}^{LB94}[\rho(\mathbf{r},t)] = V_{xc}^{LDA}[\rho(\mathbf{r},t)] - \frac{2^{1/3}\beta\chi^2(\mathbf{r})\rho^{1/3}(\mathbf{r})}{1+3\cdot 2^{1/3}\beta\chi(\mathbf{r})\sinh^{-1}\left[2^{1/3}\chi(\mathbf{r})\right]}. \quad (4)$$

Here, $V_{xc}^{LDA}[\rho(\mathbf{r},t)]$ is the exchange-correlation potential in the local density approximation [17], $\chi(\mathbf{r}) = |\nabla\rho(\mathbf{r})|/\rho^{4/3}(\mathbf{r})$, and $\beta = 0.05$. The initial condition corresponds to the ground state of the atom, which is described by the stationary Kohn-Sham orbitals $\psi_{n,0}(\mathbf{r})$:

$$\hat{H}_0\psi_{n,0}(\mathbf{r}) = E_n\psi_{n,0}, \quad \hat{H}_0 = -\frac{1}{2}\nabla^2 - \frac{Z}{r} + V_{ee}[\rho_0(\mathbf{r})], \quad (5)$$

where E_n is the energy of the *n*-th orbital.

Using TDKS orbitals and Ehrenfest's theorem one can find the time-dependent dipole acceleration of the atomic system [18]:

$$\mathbf{a}(t) = -N\mathbf{E}(t) - \int d^3r \frac{Z\mathbf{r}}{r^3}\rho(\mathbf{r},t). \quad (6)$$

Then, the macroscopic electron current density in the produced plasmas can be found as $\mathbf{j}(t) = -N_g\int_{-\infty}^{t}\mathbf{a}(t')dt'$, where N_g is the gas density before the start of the ionization process [20]. In addition, using the wave functions of TDKS orbitals after the passage of the laser pulse, one can find the final photoelectron momentum distribution [15]

$$P(\mathbf{p}) = 2\sum_{n=1}^{N/2}\left|\tilde{\psi}_n(\mathbf{p})\right|^2, \quad (7)$$

where $\mathbf{p}$ is the momentum vector and $\tilde{\psi}_n(\mathbf{p})$ is the spatial Fourier transform of the *n*-th TDKS orbital except the projections on atomic bound states.

2. THE NUMERICAL IMPLEMENTATION

2.1. THE NUMERICAL METHOD

For the numerical solution of TDKS equations, orbitals $\psi_n(\mathbf{r},t)$ are decomposed into spherical harmonics

$$Y_{lm}(\theta,\varphi) = \sqrt{\frac{(2l+1)(l-m)!}{4\pi(l+m)!}}P_l^m(\cos\theta)e^{im\varphi}, \quad (8)$$

where θ is the polar angle with respect to *z*-axis directed along the external field, φ is the azimuthal angle, P_l^m are the associated Legendre polynomials. The initial Kohn-Sham orbitals correspond to the electronic configuration of the unperturbed atom and are given by

$$\psi_{n,0}(r,\theta,\varphi) = r^{-1}\Psi_{n,0}(r)Y_{l_n m_n}(\theta,\varphi), \quad (9)$$

where l_n and m_n are orbital and magnetic quantum numbers of the *n*-th orbital. Since the external electric field has linear polarization, the magnetic quantum number of each orbitals is conserved in time, therefore in the decomposition of TDKS orbitals only the term with $m = m_n$ exists:

$$\psi_n(r,\theta,\varphi,t) = r^{-1}\sum_{l=0}^{\infty}\Psi_{nl}(r,t)Y_{lm_n}(\theta,\varphi). \quad (10)$$

To find the time dynamics of the radial component of the *n*-th TDKS orbital, the following method is used (the modification of which is also used to calculate stationary orbitals). The potential of the electron-electron interaction V_{ee} is decomposed into spherical harmonics up to the quadrupole term:

$$V_{ee}(r,\theta,t) \approx V_{ee}^{(0)}(r,t) + V_{ee}^{(1)}(r,t)\cos\theta + V_{ee}^{(2)}(r,t)\frac{1}{2}\left(3\cos^2\theta - 1\right). \quad (11)$$

Substituting (10), (11) into (1), multiplying by the spherical harmonic Y_{lm_n}, and integrating over the solid angle, we obtain a system of equations on Ψ_{nl}, which is conveniently represented in the matrix form

$$i\frac{\partial}{\partial t}\boldsymbol{\Psi}_n(r,t) = \left(\hat{\mathbf{R}}_n + \hat{\mathbf{W}}_n\right)\boldsymbol{\Psi}_n(r,t). \quad (12)$$

Here $\boldsymbol{\Psi}_n$ is the coulomn vector whose *l*-th element is Ψ_{nl}, $\hat{\mathbf{R}}_n$ is the diagonal matrix with elements

$$\left[\hat{\mathbf{R}}_n\right]_{ll} = -\frac{1}{2}\frac{\partial^2}{\partial r^2} + \frac{l(l+1)}{2r^2} - \frac{Z}{r} + V_{ee}^{(0)}(r,t) + \frac{l(l+1)-3m_n^2}{(2l-1)(2l+3)}V_{ee}^{(2)}(r,t). \quad (13)$$

The elements of the pentadiagonal matrix $\hat{\mathbf{W}}_n$, which represents the dipole interaction electrons with the electric field and dipole and partly quadrupole terms of electron-electron interaction, are given by

$$\left[\hat{\mathbf{W}}_n\right]_{kl} = \begin{cases} d_{l-2,m_n}V_{ee}^{(2)}(r,t), & k = l-2 \\ c_{l-1,m_n}\left(rE(t) + V_{ee}^{(1)}(r,t)\right), & k = l-1 \\ c_{l,m_n}\left(rE(t) + V_{ee}^{(1)}(r,t)\right), & k = l+1 \\ d_{l,m_n}V_{ee}^{(2)}(r,t), & k = l+2 \\ 0 & \text{otherwise,} \end{cases} \quad (14)$$

where

$$c_{l,m} = \sqrt{\frac{(l+1)^2 - m^2}{(2l+1)(2l+3)}}, \quad d_{l,m} = \frac{3}{2}c_{l,m}\sqrt{\frac{(l+2)^2 - m^2}{(2l+3)(2l+5)}}. \quad (15)$$

The evolution of TDKS orbitals to the time step Δt is performed using the following propagator:

$$\boldsymbol{\Psi}_n(r,t+\Delta t) = \hat{\mathbf{U}}_n(t+\Delta t,t)\boldsymbol{\Psi}_n(r,t), \quad \hat{\mathbf{U}}_n(t+\Delta t,t) = \exp\left(-i\int_t^{t+\Delta t}dt'[\hat{\mathbf{R}}_n(t') + \hat{\mathbf{W}}_n(t')]\right). \quad (16)$$

The propagator $\hat{\mathbf{U}}_n(t+\Delta t,t)$ is approximated up to the second order in Δt as follows:

$$\hat{\mathbf{U}}_n(t+\Delta t,t) \approx \exp\left(-i\Delta t\,\hat{\mathbf{W}}_n(t)/2\right) \times \exp\left(-i\Delta t\hat{\mathbf{R}}_n(t)\right)\exp\left(-i\Delta t\,\hat{\mathbf{W}}_n(t)/2\right). \quad (17)$$

The application of the exponential operator $\exp\left(-i\Delta t\hat{\mathbf{W}}_n/2\right)$ is performed using diagonalization of the matrix $\hat{\mathbf{W}}_n$ by the unitary transformation $\hat{\mathbf{W}}_n = \hat{\mathbf{S}}_n\hat{\mathbf{W}}_{n,\text{diag}}\hat{\mathbf{S}}_n^{\dagger}$, where the sign "†" corresponds to the Hermitian conjugation, resulting in

$$\exp\left(-i\Delta t\,\hat{\mathbf{W}}_n(t)/2\right) = \hat{\mathbf{S}}_n\exp\left(-i\Delta t\,\hat{\mathbf{W}}_{n,\text{diag}}(t)/2\right)\hat{\mathbf{S}}_n^{\dagger}. \quad (18)$$

The operator $\exp\left(-i\Delta t\hat{\mathbf{R}}_n\right)$ can be applied using the Crank-Nicholson approximation

$$\exp(-i\Delta t\hat{\mathbf{R}}_n) \approx (1+i\Delta t\,\hat{\mathbf{R}}_n/2)^{-1}(1-i\Delta t\,\hat{\mathbf{R}}_n/2). \qquad (19)$$

The second derivative in $\hat{\mathbf{R}}_n$ is computed using the Numerov approximation with the equidistant step along r. To calculate the radial part $\Psi_{n,0}(r)$ of the stationary Kohn-Sham orbitals (the initial condition for the time problem), we use a similar algorithm in which the time has purely imaginary values [21].

2.2. PARALLELIZATION OF NUMERICAL CODE

The method used to solve TDKS equations is well suited for execution on computer clusters, since it has two levels of parallelism. The first level is related to the properties of the matrices $\hat{\mathbf{R}}_n$ and $\hat{\mathbf{W}}_n$. The matrix $\hat{\mathbf{R}}_n$ is diagonal and the application of the operator (19) is calculated independently for each *l*-th component of the vector $\mathbf{\Psi}_n$ (*l* parallelism). The operator (18) is applied independently for each point of the radial grid (*r* parallelism). The first level of parallelism is convenient for implementing on systems with shared memory using OpenMP technology. The second level of parallelism is ensured by the fact that some operations for different orbitals are performed independently (*n* parallelism). This level of parallelism can be implemented for systems with a distributed memory using MPI technology.

For cluster systems having many nodes consisting of several sockets the parallel propagation algorithm for one time step can be implemented as follows:

- For each orbital $\mathbf{\Psi}_n(t)$ the action operator $\hat{\mathbf{U}}_n(t+\Delta t,t)$ is performed in parallel inside different sockets of different nodes of the cluster.
- The calculated values $\mathbf{\Psi}_n(t+\Delta t)$ are sent to the one (main) node.
- On the main node the electron-electron potential $V_{ee}[\rho(t+\Delta t)]$ is calculated on the basis of $\mathbf{\Psi}_n(t+\Delta t)$ and is sent to all the involved cluster nodes.

The Table compares the propagation time for one time step without using parallelization (on a single core) and using different variants of parallelization of program modules on a computer cluster. The latter consists of a large number (more than 30) nodes connected by a high-speed computer-network InfiniBand with the bandwidth 14 Gbit/s between nodes. Each node represents a two-socket system with two 10-core Intel Xeon E5-2680 v2 processors. Calculations are performed for three different noble gas atoms: neon, argon, and krypton. To describe the dynamics of the atom (using the symmetry in the spin and in the magnetic quantum number) only 4, 7, and 13 independent TDKS orbitals are used for Ne, Ar, and Kr, respectively. The radial numerical grid has N_r=10^4 nodes and the maximum value of the orbital angular momentum is $l_{\max}$=512.

As one can see from the Table, the usage of *l* and *r* parallelisms inside one socket leads to a multiple decrease of propagation time. The increase of the performance approximately equals to the number of cores in the socket (which is 10 on the used system).

Atom	One-step calculation time (s)		
	single core (no parallelism)	single socket (*r*,*l* parallelism)	cluster (*n*,*r*,*l* parallelism)
Ne	26.6	3.31	1.22
Ar	46.48	5.86	1.32
Kr	113.74	16.12	1.5

The one-time-step propagation time for three atoms: Ne, Ar, and Kr. The first column shows the result for the single-CPU (parallelization-free) calculation. The second column is propagation time for 10 cores of single processor with the parallelization of operators (18) and (19). The third column shows the propagation time with the additional parallelization in orbitals. It is computed on 2 cluster nodes for Ne, 4 nodes for Ar, and 7 nodes for Kr (each node has 20 cores in total)

At the same time, the efficiency of *n* parallelism strongly depends on the speed of data transfer between cluster nodes, on the number of sockets on each node, and on the number of independent orbitals in an atom. For the used computer cluster with 2 sockets on each node the increase of the performance is 2.7 for Ne atom, 4.4 for Ar, and 10.7 for Kr. The one-step propagation time for different atomic systems is approximately the same (1.2…1.5 s), which is associated with almost complete parallelization in orbitals.

It should be noted, however, that in the considered example the number of numerical grid nodes N_r is fixed. At the same time, when solving some physical problem with the use of TDKS equations, it is necessary to reduce the coordinate step near the nucleus as the nuclear charge increases in order to ensure high accuracy of calculations. Moreover, it is necessary also to decrease the time step Δt to resolve the natural frequencies of the lowest orbitals [22]. This leads to a rather significant decrease in the speed of numerical simulation with the increase of the atom nuclear charge, which will be demonstrated in the examples of calculation below.

2.3. EXAMPLES OF CALCULATION

In order to test the developed computational code, we consider neon, argon, and krypton atoms interacting with a few-cycle laser pulse with the electric field having the sine-squared envelope located at $0 \le t \le \tau_p$:

$$\begin{cases} E(t) = -\partial A/\partial t, \\ A(t) = -(E_0/\omega_0)\sin^2\left(\pi t/\tau_p\right)\sin(\omega_0 t). \end{cases} \qquad (20)$$

Here, E_0 is the peak amplitude of the electric field, corresponding to the peak intensity $3\cdot10^{14}$ W/cm^2, $\omega_0 \approx 0.057$ au is the carrier frequency, corresponding to the wavelength 800 nm, and $\tau_p \approx 14.7$ fs corresponds to two cycles at the full-width at half maximum of intensity.

Calculations are performed in the spatial region $0 \le r \le r_{\max}$, where $r_{\max}$ =200 au with the maximum value of the orbital angular momentum $l_{\max}$=512. The step along the radial coordinate is $\Delta r = 0.04$ au for Ne, $\Delta r = 0.02$ au for Ar, and $\Delta r = 0.01$ au for Kr, the time step is $\Delta t = 2.4\cdot10^{-2}$ au for Ne, $\Delta t = 8\cdot10^{-3}$ au for Ar, and $\Delta t = 2\cdot10^{-3}$ au for Kr. To absorb waves approaching the boundary along *r*, a three-hump imaginary potential [23] with a total width of the absorbing layer $l_{\text{abs}} = 50$ is

used. To perform the calculations we use 4 sockets/2 nodes for Ne, 7 sockets/4 nodes for Ar, and 13 sockets/7 nodes for Kr. The large difference in $N_r = r_{max}/\Delta r$ and in the time step Δt for different atoms leads to a difference in calculation time which is 5 hours for Ne, 32 hours for Ar, and 12 days 6 hours for Kr.

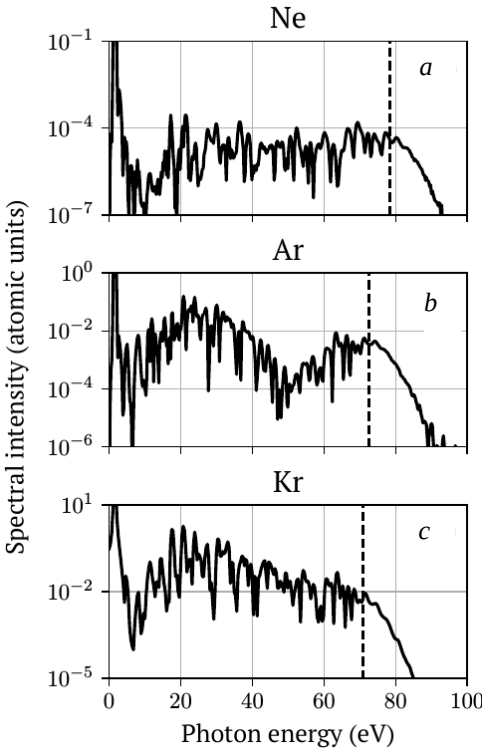

The spectra of dipole acceleration excited during interaction of Ne (a), Ar (b), and Kr (c) atoms with short laser pulse with the wavelength of 800 nm and peak intensity of $3 \cdot 10^{14}$ *W/cm*^{2}*. The dashed line indicates classical cutoff of frequency* $\omega_c = I_p + 3.17U_p$*, where* I_p *is the ionization potential of atom and* U_p *is the maximum electron ponderomotive energy*

The squared modulus of the Fourier spectrum of the dipole acceleration is shown in Figure. As can be seen from the Figure, the spectrum for Ne, Ar, and Kr contains a high-frequency part lying in the vacuum ultraviolet range, which is associated with rescattering of the photoelectrons on the parent ion [2 - 8]. The shape of the spectrum depends strongly on the type of atom. With increasing ionization potential I_p ($I_p = 13.99$ eV for Kr, 15.76 eV for Ar, and 21.55 eV for Ne), the maximum energy of the generated harmonics increases according to the well-known formula for the plateau cutoff position $\omega_c = I_p + 3.17U_p$, where U_p is the maximum electron ponderomotive energy [2, 3]. At the same time the spectral intensity decreases with increasing of ionization potential, since ionization probability of the atom decreases. The high-frequency spectrum for the case of Ar contains a minimum located approximately at 51 eV. This minimum is called Cooper minimum and is occurred due to the interference of two electron recombination channels in the ground state: $s \to p$ and $d \to p$ [6, 24]. The minimum position obtained in the presented calculation is in good agreement with the results of experiments on the high harmonics generation in Ar [24], as well as with known results of numerical calculations using the time-dependent density functional theory [18], which confirms the high accuracy of the developed code. The Cooper minimum for Kr is not observed in Figure since it is located at 80 eV [25] that is higher than the cutoff frequency ω_c for the considered parameters of the laser pulse.

CONCLUSIONS

The parallel program code has been developed for the numerical solution of the time-dependent Kohn-Sham equations for *ab initio* modeling of the evolution of many-electron atoms during the interaction with an intense laser field. The solution algorithm is based on the decomposition of the wave functions of the Kohn-Sham orbitals and the potential energy into spherical harmonics. The high accuracy of the program is demonstrated by the example of calculating the spectrum of a high-frequency electron current excited during ionization of noble gas atoms by a few-cycle laser pulse. It is shown that the use of parallelization between the nodes of modern computer clusters and between the CPUs of individual socket makes it possible to perform calculations for typical parameters of laser pulses in a relatively small time from several hours to several days depending on the atomic system under consideration.

ACKNOWLEDGEMENT

This work was supported by the Russian Science Foundation through Grant No. 17-12-01574.

REFERENCES

1. W. Becker, F. Grasbon, R. Kopold, D. Milošević, G. Paulus, H. Walther. Above-threshold ionization: From classical features to quantum effects // *Advances in Atomic, Molecular, and Optical Physics*. 2002, v. 48, p. 35-98.
2. P.B. Corkum. Plasma perspective on strong field multiphoton ionization // *Physical Review Letters*. 1993, v. 71, p. 1994.
3. M. Lewenstein, P. Balcou, M.Y. Ivanov, A. L'huillier, P.B. Corkum. Theory of high-harmonic generation by low-frequency laser fields // *Physical Review A*.1994, v. 49, p. 2117.
4. A.V. Kim, M.Y. Ryabikin, A.M. Sergeev. From femtosecond to attosecond pulses // *Physics-Uspekhi*. 1999, v. 42, p. 54-61.
5. F. Krausz, M. Ivanov. Attosecond physics // *Reviews of Modern Physics*. 2009, v. 81, p. 163.
6. M.V. Frolov, N.L. Manakov, T.S. Sarantseva, M.Yu. Emelin, M.Yu. Ryabikin, A.F. Starace. Analytic description of the high-energy plateau in harmonic generation by atoms: can the harmonic power increase with increasing laser wavelengths? // *Physical Review Letters*. 2009, v. 102, p. 243901.
7. D. Shafir, B. Fabre, J. Higuet, H. Soifer, M. Dagan, D. Descamps, E. Mével, S. Petit, H.J. Wörner, B. Pons, et al. Role of the ionic potential in high harmonic generation // *Physical Review Letters*. 2012, v. 108, p. 203001.
8. H.-C. Wu, J. Meyer-ter Vehn. Giant half-cycle attosecond pulses // *Nature Photonics*. 2012, v. 6, p. 304.

9. K.-Y. Kim, A.J. Taylor, J.H. Glownia, G. Rodriguez. Coherent control of terahertz supercontinuum generation in ultrafast laser-gas interactions // *Nature photonics.* 2008, v. 2, p. 605-609.
10. A.A. Silaev, N.V. Vvedenskii. Residual-current excitation in plasmas produced by few-cycle laser pulses // *Physical Review Letters.* 2009, v. 102, p. 115005.
11. N.V. Vvedenskii, A.I. Korytin, V.A. Kostin, A.A. Murzanev, A.A. Silaev, A.N. Stepanov. Two-color laser-plasma generation of terahertz radiation using a frequency-tunable half harmonic of a femtosecond pulse // *Physical Review Letters.* 2014, v. 112, p. 055004.
12. T. Balciunas, D. Lorenc, M. Ivanov, O. Smirnova, A. Zheltikov, D. Dietze, K. Unterrainer, T. Rathje, G. Paulus, A. Baltuška, et al. CEP-stable tunable THz-emission originating from laser-waveform-controlled sub-cycle plasma-electron bursts // *Optics Express.* 2015, v. 23, p. 15278-15289.
13. V.A. Kostin, I.D. Laryushin, A.A. Silaev, N.V. Vvedenskii. Ionization-induced multiwave mixing: Terahertz generation with two-color laser pulses of various frequency ratios // *Physical Review Letters.* 2016, v. 117, p. 035003.
14. A.A. Silaev, V.A. Kostin, I.D. Laryushin, N.V. Vvedenskii. Ionization mechanism of the generation of tunable ultrashort pulses in the mid-infrared range // *JETP Letters.* 2018, v. 107, p. 151-156.
15. U. De Giovannini, D. Varsano, M.A. Marques, H. Appel, E.K. Gross, A. Rubio. Ab initio angle- and energy-resolved photoelectron spectroscopy with time-dependent density-functional theory // *Physical Review A.* 2012, v. 85, p. 062515.
16. S.-I. Chu. Recent development of self-interaction-free time-dependent density-functional theory for nonperturbative treatment of atomic and molecular multiphoton processes in intense laser fields // *The Journal of Chemical Physics.* 2005, v. 123, p. 062207.
17. C.A. Ullrich. Time-dependent density-functional theory: concepts and applications // *Oxford graduate texts, Oxford University Press*. 2011.
18. D.A. Telnov, K.E. Sosnova, E. Rozenbaum, S.-I. Chu. Exterior complex scaling method in time-dependent density-functional theory: Multiphoton ionization and high-order-harmonic generation of Ar atoms // *Physical Review A.* 2013, v. 87, p. 053406.
19. R. Van Leeuwen, E. Baerends. Exchange-correlation potential with correct asymptotic behavior // *Physical Review A.* 1994, v. 49, p. 2421.
20. A.A. Silaev, M.Y. Ryabikin, N.V. Vvedenskii. Strong-field phenomena caused by ultrashort laser pulses: Effective one- and two-dimensional quantum-mechanical descriptions // *Physical Review A.* 2010, v. 82, p. 033416.
21. D. Bauer, P. Koval. Qprop: A Schrödinger-solver for intense laser-atom interaction // *Computer Physics Communications*. 2006, v. 174, p. 396-421.
22. A. Castro, M.A. Marques, A. Rubio. Propagators for the time-dependent Kohn-Sham equations // *The Journal of Chemical Physics.* 2004, v. 121, p. 3425-3433.
23. A.A. Silaev, A.A. Romanov, N.V. Vvedenskii. Multi-hump potentials for efficient wave absorption in the numerical solution of the time-dependent Schrödinger equation // *Journal of Physics B: Atomic, Molecular and Optical Physics.* 2018, v. 51, p. 065005.
24. H.J. Wörner, H. Niikura, J.B. Bertrand, P.B. Corkum, D.M. Villeneuve. Observation of electronic structure minima in high-harmonic generation // *Physical Review Letters.* 2009, v. 102, p. 103901.
25. A.D. Shiner, et al. Probing collective multi-electron dynamics in xenon with high-harmonic spectroscopy // *Nature Physics*. 2011, v. 7, p. 464.

Article received 01.07.2018

КВАНТОВО-МЕХАНИЧЕСКОЕ МОДЕЛИРОВАНИЕ ВЗАИМОДЕЙСТВИЯ МНОГОЭЛЕКТРОННЫХ КВАНТОВЫХ СИСТЕМ С ИОНИЗИРУЮЩИМИ ЛАЗЕРНЫМИ ИМПУЛЬСАМИ

А.А. Романов, А.А. Силаев, Д.А. Смирнова, Т.С. Саранцева, А.А. Минина, М.В. Фролов, Н.В. Введенский

Разрабатывается параллельный программный код для численного моделирования взаимодействия интенсивных лазерных импульсов с многоэлектронными атомами на основе нестационарного метода функционала плотности. Показывается, что использование современных многопроцессорных вычислительных кластеров позволяет решить нестационарные уравнения Кона-Шэма для широкого класса атомов за относительно небольшое время, определяемое параметрами лазерного импульса и электронной конфигурацией атома. Демонстрация работы численного кода представлена на примере расчета спектра высокочастотного электронного тока, возбуждаемого при ионизации атомов инертных газов коротким лазерным импульсом.

КВАНТОВО-МЕХАНІЧНЕ МОДЕЛЮВАННЯ ВЗАЄМОДІЇ БАГАТОЕЛЕКТРОННИХ КВАНТОВИХ СИСТЕМ З ІОНІЗУЮЧИМИ ЛАЗЕРНИМИ ІМПУЛЬСАМИ

А.А. Романов, А.А. Силаєв, Д.А. Смирнова, Т.С. Саранцева, А.А. Мініна, М.В. Фролов, Н.В. Введенський

Розробляється паралельний програмний код для чисельного моделювання взаємодії інтенсивних лазерних імпульсів з багатоелектронними атомами на основі нестаціонарного методу функціонала щільності. Показується, що використання сучасних багатопроцесорних обчислювальних кластерів дозволяє розв'язати нестаціонарні рівняння Кона-Шема для широкого класу атомів за відносно невеликий час, що визначається параметрами лазерного імпульсу і електронною конфігурацією атома. Демонстрація роботи чисельного коду представлена на прикладі розрахунку спектра високочастотного електронного струму, що збуджується при іонізації атомів інертних газів коротким лазерним імпульсом.